Vol. 15, No. 3 (2016) 763-771
Revista Mexicana de Ingeniería Química

A MATHEMATICAL MODEL OF THE OSCILLATIONS OF pH FOR THE ANODIC BIOFILM FORMATION IN A MICROBIAL FUEL CELL

MODELO MATEMÁTICO DE LAS OSCILACIONES DE pH PARA LA FORMACIÓN DE LA BIOPELÍCULA ANÓDICA EN UNA CELDA DE COMBUSTIBLE MICROBIANA

I. Peraza-Baeza[1], A. Perez-Hernandez[2], L. Blanco-Cocom[3], J. Domínguez-Maldonado[4], L. Alzate-Gaviria[4*]

[1]*Swette Center for Environmental Biotechnology, Biodesign Institute at Arizona State University, 1000 S. McAllister Ave., P.O. Box 875701, Tempe, AZ 85287-5701, USA*

[2]*Advanced Material Research Center (CIMAV), Computer Simulation Department. Ave. Miguel de Cervantes 120, Complejo Industrial Chihuahua, 31109 Chihuahua, Chihuahua, México.*

[3]*Mathematics Research Center (CIMAT), Jalisco, Colonia Valenciana, 36023, Guanajuato, Guanajuato, México.*

[4]*Yucatan Center for Scientific Research (CICY), Renewable Energy Unit. Calle 43 No. 130, Colonia Chuburná de Hidalgo, 97200 Mérida, Yucatán, México.*

Recibido 1 de Enero de 2016; Aceptado 26 de Junio de 2016

Abstract

This paper presents a mathematical model developed in order to predict the anodic biofilm growth, considering the oscillatory behavior of the pH in the anodic chamber and the microbial kinetics. The kinetic parameters were estimated using a modified genetic algorithm. The results obtained by simulations provide a good fitting to the experimental data, indicating an optimum pH of 7.12 and q_{max} = 0.15 g Ac g X^{-1} day^{-1}. The anodic biofilm shows slow growth kinetics, meaning that the substrate concentration gradients were important up until the final stage of growth and showing prevalence of active biomass up to 22 micrometers away from the electrode. The increase of the current density obtained is associated with the increase of the biofilm thickness.

Keywords: microbial fuel cell, anodic biofilm, modeling, waste treatment.

Resumen

En este trabajo se presenta un modelo matemático desarrollado para predecir el crecimiento de biopelículas anódicas, teniendo en cuenta el comportamiento oscilatorio del pH anódico y la cinética microbiana. Los parámetros cinéticos se estimaron utilizando un algoritmo genético modificado. Los resultados en las simulaciones proporcionan un buen ajuste a los datos experimentales, se indica un pH óptimo de 7.12 y q_{max} = 0.15 g Ac g X^{-1} day^{-1}. La biopelícula anódica muestra una cinética de crecimiento lento, lo que significa que los gradientes de concentración de sustrato fueron importantes hasta la etapa final de crecimiento y que muestra la prevalencia de la biomasa activa hasta 22 micrómetros de distancia desde el electrodo. El aumento de la densidad de corriente se asocia con el aumento del espesor de la biopelícula.

Palabras clave: celda de combustible microbiana, biopelícula anódica, modelado, tratamiento de residuos.

1 Introduction

In Microbial Fuel Cells (MFC) there are still technical challenges whose identification and solution will allow for improvement in the efficiency of the system. The behavior of a MFC is strongly influenced by diverse physical, chemical and biological factors like the mass transfer in the biofilm, microbial oxidation of the substrate, electron transfer from the microorganisms to the electrode, diffusion of ions through the cell chambers etc. (Picioreanu *et al*., 2010, Domínguez-Maldonado *et al*., 2014). Current studies about MFCs are still mainly experimental, and focus on a detailed description of the microbiology of the involved bacteria or the engineering aspects (Valdez-Ojeda *et al*., 2014). More than a decade ago, a preliminary work tried to simulate the electric current generated for a MFC using suspended cells and electron shuttles (Zhang *et al*., 1995). This research field stopped until 2007 when Picioreanu

* *Corresponding author. E-mail*: lag@cicy.mx
Tel.: +52 (999) 942 83 30; fax: +52 (999) 981 39 00.

and his team introduced the biofilm-based microbial fuel cell model that incorporates mediated electron transfer (Picioreanu *et al*., 2007). Using a different hypothesis, Kato-Marcus explained the functionality of the anode respiring bacteria biofilm considering that it has conductive properties instead of electron mediators, using the Nernst-Monod equation (Marcus *et al*., 2007). On the other hand, there are only a couple of modeling studies that consider the dynamics of pH on the electrochemical behavior of the MFC, even when its importance over the reversible electrochemical oxidation and the microbial activity are key elements on the biofilm evolution. The main objective of this work was the development of a mathematical model to describe the oscillatory changes of the anodic pH and its relationship with the electrochemical behavior of the MFC, since many studies indicated that the acidification of the anolyte is a key limitation that impedes the employment of the MFC based technologies (Korth *et al*., 2015, Picioreanu *et al*., 2010, Torres *et al*., 2010).

2 Materials and methods

2.1 MFC setup and operation

Information on MFC preparation, inoculation, setup and operation can be found at Sanchez *et al*., (2014).

2.2 Definition of the mathematical model

The mathematical model considers the mass balance of microorganisms and substrates which are involved in the electrical energy production by the cell while describing the bacterial growth dynamics, substrate consumption, and electricity generation, considering the pH as a main operation parameter. Later, with the estimated parameters a simulation of the anodic biofilm growth was developed (Figure 1). The model assumes the following:

a) A mix consortium of bacteria growth in the anodic chamber following Monod double saturation kinetics and generating electrical current.

b) The electrical current depends on the concentration of bacteria and the specific substrate consumption rate (q).

c) The substrate consumption rate of the donor (q) depends on the substrate concentration (S) and the pH of the solution.

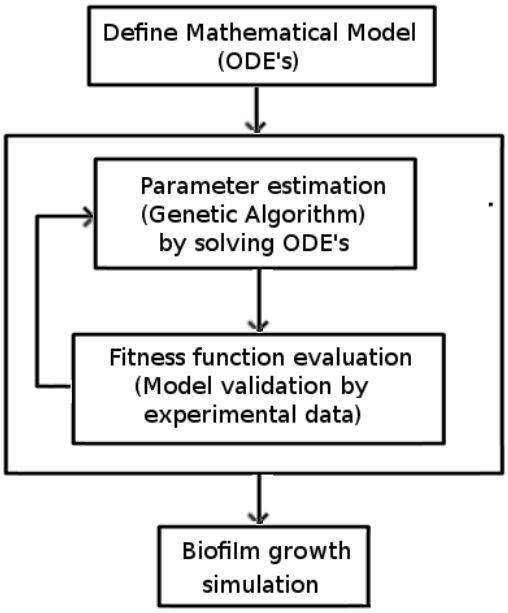

Fig. 1. General framework of the modeling process.

d) A dual electron transfer mechanism governed by intracellular mediators excreted by bacteria and electrical conductive nanowires is assumed.

3 Results and discussion

3.1 Electrical current

The first step of the modeling process was the conversion of the experimental data of electrical current to substrate concentration units, for which the equation defined by Logan *et al*. (2006) was used and solved for dS/dt.

$$\frac{dS}{dt} = \frac{M_S IA}{CEFnV} \tag{1}$$

Where, M_s = molecular weight (g mol^{-1}), I = current density (A m^{-2}), A=area of the electrode (m^2), t = time of the experiment (s), S = substrate concentration (g L^{-1}), n = number of mol of electrons per mol of substrate, F is the Faraday constant (96,485 C mol^{-1} or A s mol^{-1}), V = volume of the anodic chamber (m^3), CE is the coulombic efficiency assumed to be 50 % a common value for MFCs (Logan *et al*., 2008). The substrate consumption kinetics of the cell is directly related to the bacteria concentration (Logan *et al*., 2006).

3.2 The oscillatory pH model

This model is based on the concept of an underdamped electrical circuit with an electrical charge (Q) associated with an electrical current flowing through an electrical circuit LRC (inductor, resistor and capacitor) where the sum of the drop voltages are proportional to the applied voltage, equation (2).

$$L\frac{d^2Q}{dt^2} + R\frac{dQ}{dt} + \frac{1}{C}Q = E(t) \tag{2}$$

Where, E (t) is the applied voltage. In the oscillatory pH model it was assumed that the anodic pH (pH_{An}) behaves similarly; so the electrical meaning of every element in the LRC circuit could be reinterpreted and linked to the phenomena that took place in the anodic chamber. Replacing the constants LRC for k_M^0, r^0 and $Y_{X/S}$ respectively, equation (2) gives:

$$k_m^o\frac{d^2pH}{dt^2} + r^o\frac{dpH}{dt} + \frac{1}{Y_{X/S}}pH = B(t) \tag{3}$$

Where, $k_m^0 = k_{m,OH^-}/k_{m,H^+}$; $r^0 = r_B/q$; k_{m,OH^-}= Mass transfer coefficient for hydroxyl ions across the proton exchange membrane (m/s); k_{m,H^+}= Mass transfer coefficient for protons across the PEM (m/s); r_B = reactivity of the buffer solution given by: $r_B = k_{CO_2}\left(C_{CO_2} - \frac{C_H C_{HCO_3}}{k_{CO_2}}\right)$ with units of (mol CO_2 L^{-1} day^{-1}) where K_{CO_2} is the reactivity constant of the buffer, C_{CO_2}, C_H and C_{HCO_3} are the concentrations of CO_2, protons and carbonic acid, considering the chemical reaction $CO_2 + H_2O \leftrightarrow HCO_3^- + H^+$; and B(t) is the buffer solution concentration as a function of time (g L^{-1} day^{-1}). The first term of the equation (3) expresses the tendency to the change in the pH of both chambers of the cell, caused mainly by the migration of ions from both chambers of the cell trough the membrane, including the relationship between the ion mass transfer coefficients (Rozendal *et al*., 2006). The second term expresses the changes in pH due to the buffer reactivity (r_B) in the solution, which in turn depends on the substrate consumption rate (q). Finally, the changes of the pH associated with the bacteria population were included by the parameter ($Y_{X/S}$) that is directly related to the substrate consumption. Since the differential equation is a second order, equation (4), represents an under damped oscillatory system whose analytical solution is the following:

$$pH(t) = ae^{-bt}\cos(ct + d) + pH_{opt} \tag{4}$$

Where, ae^{-bt}= pH oscillation range (amplitude); $b = k_m^0/r^o$ = relationship between the ions transfer and the buffer reactivity; $c = \sqrt{Y_{X/S}/r^0}$ = pH oscillation frequency, d = displacement angle over the x axis; pH_{opt} = pH at which the maximum substrate rate is reached (q_{max}). Later, the anodic pH kinetics was linked with q_{max}, using the inhibition function for anode respiring bacteria (ARB) adapted from equation (5) (Torres *et al*., 2010); where it is assumed that q approaches to zero, when the pH oscillates between an upper and lower limit of the optimum, (pH_{opt}).

$$q = \begin{cases} 0 & for\ pH < pH_{opt} - W \\ \frac{q_{\max}X}{2}\left[1 + \cos\left(\frac{\pi}{W}\left(pH - pH_{opt}\right)\right)\right] & for\ pH_{opt} + W > pH > pH_{opt} - W \\ q_{\max}X & for\ pH > pH_{opt} \end{cases} \tag{5}$$

Where, q_{max},X = the maximum substrate consumption rate for the bacteria (day^{-1}), pH_{opt} = pH at which $q \rightarrow q_{max}$. A specific Monod growth rate, equation (6) was also included.

$$q(pH) = \frac{q_{\max}X(t)}{2}\left[1 + \cos\left(\frac{\pi}{W}\left(pH(t) - pH_{opt}\right)\right)\right]\left(\frac{S(t)}{S(t) + K_S}\right) \tag{6}$$

Combining the equations (4) and (6), the relationship between the oscillatory pH and the substrate consumption rate is obtained.

$$q = \frac{q_{\max}X(t)}{2}\left[1 + \cos\left(\frac{\pi}{W}\left(ae^{-bt}\cos(ct + d)\right)\right)\right]\left(\frac{S(t)}{S(t) + K_S}\right) \tag{7}$$

Finally, adding the endogenous decay term, the differential equation that describes the bacteria growth kinetics as a function of the substrate concentration and the oscillatory pH (equation 8) was obtained, where k_d is the endogenous decay constant (g L^{-1}).

$$\frac{dX(t)}{dt} = \frac{q_{\max}Y_{X/S}X(t)}{2}\left[1 + \cos\left(\frac{\pi}{W}\left(ae^{-bt}\cos(ct + d)\right)\right)\right]\left(\frac{S(t)}{S(t) + K_S}\right) - k_dX(t) \tag{8}$$

3.3 Parameter estimation

The simulations of the substrate consumption, mass production and current density, were performed based on equations (1) and (8) and the experimental data. The kinetic parameters: Θ = [q_{max}, $Y_{X/S}$, W, k_d and K_S] from equation (8), were estimated through the genetic algorithm (GA) published in the work of Blanco *et al*., 2013. The algorithm used the optimization routine lsqcurvefit coupled with the Levenberg-Marquart algorithm and implemented in MATLAB in order to obtain a local estimation of the parameters of the system of differential equations that were solved through the routine ode23 where the objective function was:

$$\min \sum_{j=1}^{N} \left(y_k(j,\theta) - ydata_{k,j}\right)^2, (k = 1,2,...,M) \quad (9)$$

Where N is the number of experimental data, M is the number of differential equations in the system, $ydata_{k,j}$ is the jth experimental data associated with the differential equation k, and $y_k(j,\Theta)$ is the associated prediction with the k_{th} equation and with $ydata_{k,j}$, θ is the possible optimum solution for the set of parameters of the differential equations system.

The fitness function used in this article is:

$$f(\theta) = \frac{1}{\sum_j \left(y_k\left(t_j,\theta\right) - ydata_j\right)^2} \quad (10)$$

This function has the objective to evaluate the aptitude of each possible solution θ, in order to find the best set of parameters θ^* of the mathematical model. More details can be found in the study of Blanco *et al*. (2013).

3.4 Formulation of the biofilm model influenced by the oscillatory pH

A one dimensional mathematical model was formulated using equation (7), in order to describe the anodic biofilm thickness and the substrate and biomass concentration gradients, similar to the work of Marcus *et al*. (2007). The substrate consumption rate (q) depends on the anodic pH and the bacteria concentration (Marcus *et al*., 2011). The variable X(t) of equation (7) was changed for ϕ_a to indicate that the kinetics takes place in the biofilm.

$$q = \frac{q_{\max}\phi_a}{2}\left[1 + \cos\left(\frac{\pi}{W}\left(ae^{-bt}\cos(ct+d)\right)\right)\right]\left(\frac{S}{S+K_S}\right) \quad (11)$$

The model includes terms for endogenous respiration rate ($r_{res} = b_{res}\phi_a; day^{-1}$) and inactivation of the active biomass ($r_{ina} = b_{ina}\phi_a; day^{-1}$), where, b_{res} and b_{ina} are the decay and inactivation coefficients for the biomass specific rate (day^{-1}), respectively. In order to calculate the substrate concentration in the biofilm, we used a reaction-diffusion equation where, under stationary conditions, the consumption kinetics overlaps the concentration gradient decay over time, obtaining the equation (12):

$$0 = D_{S,f}\frac{\partial^2 S_d}{\partial z^2} - X_{f,a}q \quad (12)$$

Where, $D_{S,f}$ is the substrate diffusion coefficient in the biofilm ($cm^2\ day^{-1}$) and $X_{f,a}$ is the active biomass density ($g\ L^{-1}$). A diffusion coefficient in the biofilm of about 80 % of the diffusion coefficient in the bulk was used according to Marcus *et al*. (2011).

3.5 Biofilm growth and distribution

Following the methodology of Marcus *et al*. (2007), the active and inactive biomass fractions in the biofilm were represented with the terms ϕ_a and ϕ_i, respectively. The biomass balances were calculated using a relationship with the detachment velocity (u) with the growth rate of every type of biomass,

$$\frac{\partial u}{\partial z} = \mu_a + \mu_i \quad (13)$$

Where, μ_a and μ_i are the detachment velocities in every point, z of the biofilm, and can be determined integrating the equation (14) from zero to z´ (Marcus *et al*., 2007):

$$u(t,z') = \int_0^{z'} (\mu_a + \mu_i)dz \quad (14)$$

Hence, the biofilm thickness changes in relation to the detachment velocity,

$$\frac{dL_f}{dt} = u(t,L_f) - b_{des}L_f \quad (15)$$

Where, L_f is the anodic biofilm thickness (μm). The second term of equation (15) indicates the detachment velocity of the biomass. Table 1 shows the parameters employed for the biofilm model simulation. The diffusion coefficient values were taken from (Marcus *et al*., 2007).

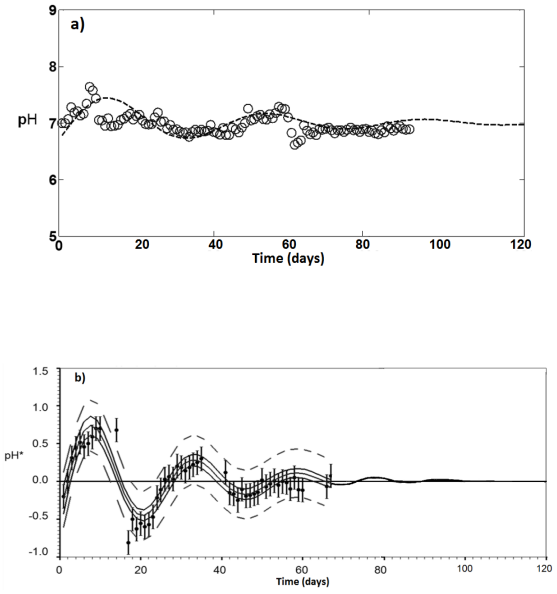

Fig. 2. a) Average anodic pH as a function of time for experimental data, showing an oscillatory behavior of the system, b) Fitting curve for the experimental data of pH* for one single MFC over time using the software LabFit^{TM}, the selection of one single cell was based on the observance of a similar behavior of the other reactors.

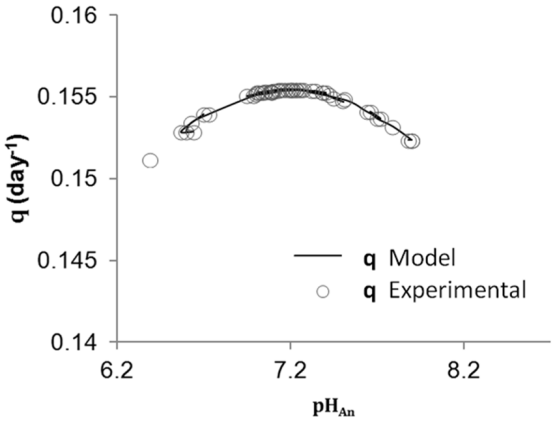

Fig. 3. Comparison of the experimental data for the curve of q vs anodic pH (pHAn) and the simulation, the empty blue circles represent the experimental data and the solid line, the simulation using the equation (5).

Simulations of the biofilm growth model were made in the biofilm reactor compartment simulator of AQUASIM^{TM} 2.1d program, demo version developed by (EAWAG).

3.6 Simulation of the anodic pH oscillations

Figure 3 shows the average of the experimental pH values for 2 MFCs fitted with the model. Decreasing oscillations over time can be observed because of the tendency of the system to reach an optimum and stable pH. The pH oscillations in MFC have been reported previously, indicating that they are originated mainly by: a) ion transfer through the membrane from both chambers of the cells, b) the reactivity of the buffer in the bulk and in the biofilm and c) substrate concentration that affects the parameters q and $Y_{X/S}$, (Marcus *et al*., 2011, Park *et al*., 2007). In order to improve the fitting, the reference axis was moved and the oscillation midpoint described as pH* = pH_{opt} - 7.12. Picioreanu *et al*. (2010) reported this oscillation phenomenon in the pH of the anolyte, with a tendency toward the initial value. The anodic pH increased from 7 to 8.5 (during the first 10 days) possibly because of the presence of ions like Na^+ and K^+ in the inoculum and CO_2 production, that increased the bicarbonate concentration (Fanga *et al*., 2013). Later, it decreased to 6.39 (day 20) due to the generation of protons and their accumulation in the surface of the membrane (Rozendal *et al*., 2006). This behavior remained until the cell reached a stable value of 7.12. Picioreanu *et al*. (2010) also studied the effect of the anodic pH in the electricity generation, indicating that at certain proton transfer rates, an accumulation of them in the anodic chamber decreased the pH (Picioreanu *et al*., 2010). However, at a constant rate, the current was mainly limited by the biomass attached to the electrode. Other models like the one of Marcus *et al*. (2011) describe the oscillatory pH, without biofilm growth, considering a stable pH zone. Using equation 5, the pH vs q curve was determined. Figure 3 indicates that q reached a maximum of 0.15 day^{-1} with pH_{opt} = 7.12. The oscillations were greater at the beginning but they decreased since the bacteria adapted to the environment, caused by the decrease in the enzymatic reaction rates (Park *et al*., 2007).

3.7 Parameter estimation

In this study a GA, employed successfully in a previous publication on a Microbial Electrolysis Cell (Blanco *et al*., 2013), was used in order to estimate the parameters of the system presented in Table 2.

Table 1. Kinetic parameters used in the implementation of the anodic biofilm model, all the parameters were estimated using the genetic algorithm method.

Symbol	Value	Units	Reference
q_{max}	0.150	mol S g day^{-1}	Estimated
K_S	0.084	mol S cm^{-3}	Estimated
W	1.298	pH	Estimated
Y	1.002	mol X mol S^{-1}	Estimated
S_{liq}	0.085	mol S cm^{-3}	Experimental

The value of q_{max} at the beginning was 0.15 day^{-1} and increased due to the tendency of the system to reach optimum growth conditions for the bacteria (Marcus *et al*., 2007). Other simulation studies show that q_{max} is greater due to the use of parameters of *G. Sulfurreducens* that have greater consumption rates than those of mixed cultures (Picioreanu *et al*., 2007). The coefficient $Y_{X/S}$, began with a value of 0.59 and increased to 2.26 because of the increase of the substrate consumption and growth rate (Lee *et al*., 2008), coinciding with the increasing of q_{max}. Finally, $Y_{X/S}$ decreased to 1.02, allowing a continuous growth, although to a lesser extent (Marcus *et al*., 2007). The parameter W is among those reported in the literature for MFC, between 1 and 2.5 units of pH (Marcus *et al*., 2011). The endogenous decay constant kd shows a tendency to decrease, reaching similar values to the one reported by Zeng *et al*. (2010). Finally, K_S was between 0.41 and 3 g L^{-1} caused by an increase in the affinity to the substrate consumption, (Picioreanu *et al*., 2007; Pinto *et al*., 2010).

3.8 Current density simulation

Figure 4a presents the results for the anodic current density simulation using the equation (1). It shows that up to day 66, the model predicts a smaller current compared with the experimental data, probably because the model does not consider the cathodic reaction which is a limiting factor in these systems (Zeng *et al*., 2010). From day 67, the computations indicate a greater current, compared to the experimental data, showing a good fit with the corresponding values at 150 days of experimentation.

3.9 Substrate consumption and bacterial growth

Substrate consumption was maintained at an acetate concentration of 6 g L^{-1} throughout the experimental period. The simulation shows a fitting of 89 % for the substrate and bacteria curves when compared with the simulations, Figure 4(b,c). Up until day 55, the kinetics shows a limited consumption and a small increase in biomass production coinciding with the estimated parameters (Table 2). Subsequently, the substrate decreases slowly and an increase in biomass was observed. At day 66, q does not increase significantly, but the value of $Y_{X/S}$ (Table 2) does, due to competition with other bacteria that do not consume acetate (Pinto *et al*., 2010; Torres *et al*., 2007). Finally, q reaches its maximum value which coincides with the stabilization of pH, Fig. 2b.

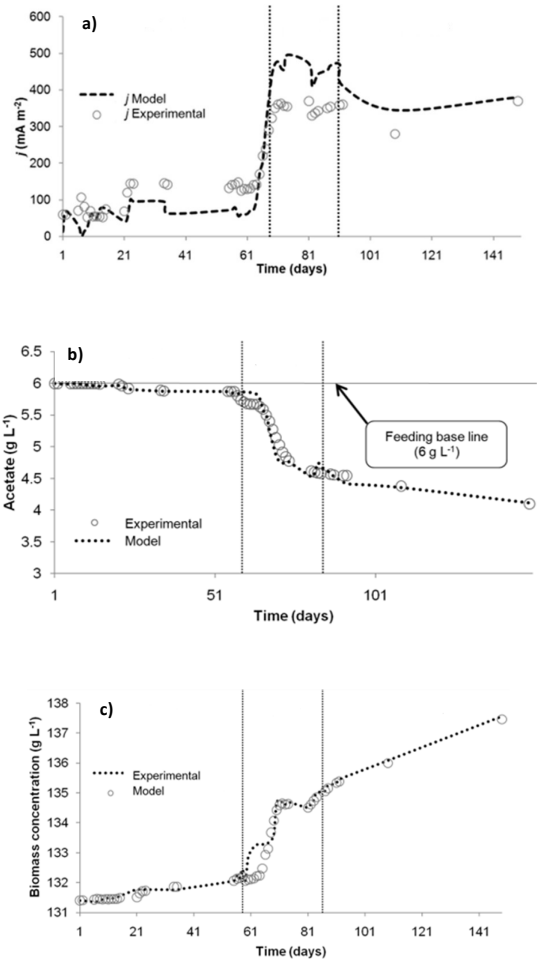

Fig. 4. Experimental and simulation data of the a) Current density generation, with an external resistance = 1000 Ω. b) Substrate consumption and c) biomass production.

Table 2. Results of the parameters estimation for the MFC, showing a comparison between the estimated parameters of the model with previous modeling studies, the units of the values were homogenized for comparison purpose.

q_{max} (day^{-1})	$Y_{X/S}$ (g X*g S^{-1})	W (pH)	k_d (g L^{-1})	Ks (g L^{-1})	Reference
0.13-4.01	0.59-2.26	1.33	5.6×10^{-3}	0.25-3.01	This study
0.13	2.26	3.33	5.0×10^{-2}	0.25	Marcus *et al*., (2010)
22.85	0.21	-	8.4×10^{-4}	0.037	Picioreanu *et al*., (2010)

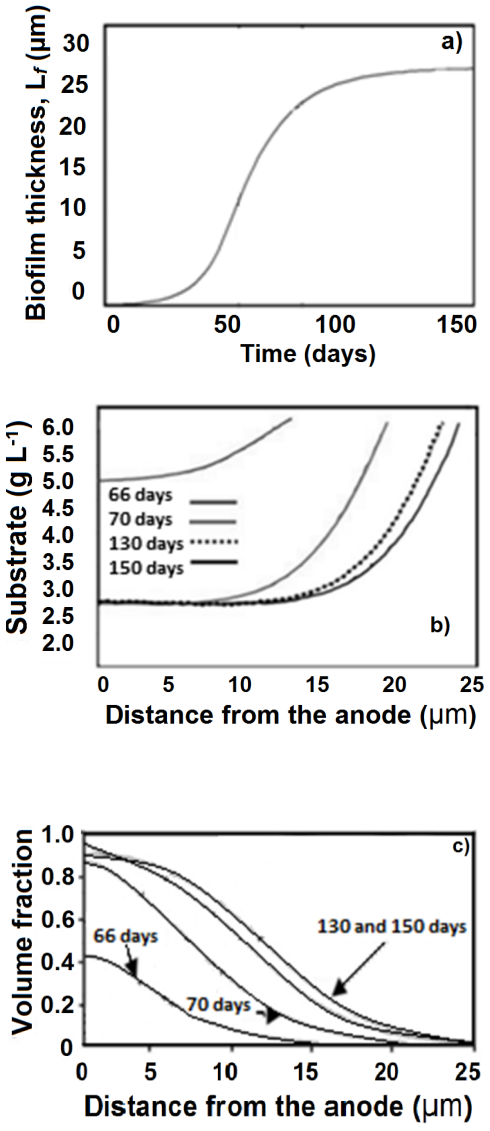

Fig. 5. Simulation results of the anodic biofilm growth. a) Evolution of the biofilm thickness at 150 days, with q = 0.05 day^{-1}. b) The steady-state profile for substrate concentration growth for 66, 70, 130 and 150 days. C) The steady-state profile for active biomass growth for 66, 70, 130 and 150 days.

3.10 Simulation of anodic biofilm growth

The simulation for the biofilm growth resulted in the accumulation of biomass in the electrode as shown, Figure 5a. Initially, the adaptation phase is shown, followed by exponential growth, as a result of the biomass growth attached to the electrode, (Lee *et al*., 2009). Finally, a stationary zone extending up to 150 days with a thickness of 25 microns, coincides with those reported by other authors, (Picioreanu *et al*., 2007; Marcus *et al*., 2007). Figure 5b shows the concentration profile of the substrate in the anodic biofilm as a function of the distance from the anode surface. In the first 66 days, the concentration decreased from 6.0 to 5.0 g L^{-1}. The presence of a smaller gradient indicates that most of the population has access to the same substrate concentration. On days 70, 130 and 150, a greater gradient is observed, caused by the increase in the biofilm thickness. The increased gradient causes an increase in current density (Marcus *et al*., 2007); a high concentration gradient restricts the availability of the substrate by the bacteria close to the electrode thereby reducing the current density. However, the current increases with time, suggesting the occurrence of conductive nanowires, which allow the growth of the biofilm and increasing the electricity generation, reducing the extracellular potential losses, (Marcus *et al*., 2007; Marcus *et al*., 2011; Gorby *et al*., 2006). Figure 5c shows the Volume fraction for the active biomass as a function of the distance from the anode surface. In the first 66 days, the volume fraction present in the biofilm was showed only up to 15 microns, at 70 days the midpoint between two types of biomass moved to 7 microns and a major prevalence of the active biomass was extended until 20 microns, which rises to 12 microns in the midpoint on days 130 and 150. The biomass corresponding to 150 days is located up to 16 microns of the electrode, showing no presence at 25 microns. Matching the results of Figures 4b and 4c, the inactive biomass increases with the biofilm thickness, due to an increased energy requirement in order to counteract the loss of extracellular potential

(Picioreanu *et al*., 2007; Marcus *et al*., 2007: Zeng *et al*., 2010).

Conclusions

The mathematical model of the electrochemical behavior of the analyzed MFC was a function of oscillatory pH, unlike other models that are successful under constant values. The genetic algorithm contributed to find the set of parameters that allowed the best fit for the experimental data, where $Y_{X/S}$, q_{max} and W, were the most important parameters in the kinetics of substrate consumption and biofilm formation. Electricity production is governed by the biofilm and fluctuating changes in the pH. This study provides a tool for prediction and control, with less invasive action to a system in development, or in continuous operation.

Acknowledgements

The authors thank the National Council for Science and Technology (CONACYT) for Grant No. 224387 awarded while conducting this research and the Yucatan Center for Scientific Research (CICY), for providing the facilities.

References

Blanco-Cocom L., Guerrero-Álvarez A., Domínguez-Maldonado J., Ávila-Vales E., Alzate-Gaviria L. (2013). Mathematical model for a continuous hydrogen production system: Stirred fermenter connected to a biocatalyzed electrolysis cell. *Biomass and Bioenergy 48*, 90-99.

Domínguez-Maldonado J.A., García-Rodríguez O., Aguilar-Vega M., Smit M., Alzate-Gaviria L. (2014). Reduction of cation exchange capacity in a microbial fuel cell and its relation to the power density. *Revista Mexicana de Ingeniería Química 13*, 527-538.

Fanga F., Zanga G., Suna M., Yua H. (2013). Optimizing multi-variables of microbial fuel cell for electricity generation with an integrated modeling and experimental approach. *Applied Energy 110*, 98-103.

Gorby Y.A., Yanina S., Mclean J.S., Rosso K.M., Moyles D., Dohnalkova A., Beveridge T.J., Chang I.S., Kim B.H., Kim K.S., Culley D.E., Reed S.B., Romine M.F., Saffarini D.A., Hill E.A., Shi L., Elias D.A., Kennedy D.W., Pinchuk G., Watanabe K., Ishii S., Logan B., Nealson K.H., Fredrickson J.K. (2006). Electrically conductive bacterial nanowires produced by Shewanella oneidensis strain MR-1 and other microorganisms. *PNAS USA 103*, 11358-11363.

Korth B., Rosa L., Harnisch F., Picioreanu C. (2015). A framework for modeling electroactive microbial biofilms performing direct electron transfer. *Bioelectrochemistry 106*, 194-206.

Lee H., Parameswaran P., Kato-Marcus A., Torres C.I., Rittmann B.E. (2008). Evaluation of energy-conversion efficiencies in microbial fuel cells (MFCs) utilizing fermentable and non-fermentable substrates. *Water Research 42*, 1501-1510.

Lee H.S., Torres C.I., Rittmann B.E. (2009). Effects of substrate diffusion and anode potential on kinetic parameters for anode-respiring bacteria. *Environmental Science & Technology 43*, 7571-7577.

Logan B.E., Hamelers B., Rozendal R., Schröder U., Keller J., Freguia S., Aelterman P., Verstraete W., Rabaey K. (2006). Microbial fuel cells: methodology and technology. *Environmental Science & Technology 40*, 5181-5192.

Marcus A.K., Torres C.I., Rittmann B.E. (2011). Analysis of a microbial electrochemical cell using the proton condition in biofilm (PCBIOFILM) model. *Bioresource Technology 102*, 253-262.

Marcus A., Torres C.I., Rittmann B. (2007). Conduction-based modeling of the biofilm anode of a microbial fuel cell. *Biotechnology & Bioengineering 98*, 1171-1182.

Park S., Bae W., Chung J., Baek S. (2007). Empirical model of the pH dependence of the maximum specific nitrification rate. *Process Biochemical 42*, 1671-1676.

Picioreanu C., Loosdrecht M., Curtis T., Scott K. (2010). Bioelectrochemistry Model based evaluation of the effect of pH and electrode geometry on microbial fuel cell performance. *Bioelectrochemistry 78*, 8-24.

Picioreanu C., Head I., Katuri K., Van Loosdrecht M., Scott K. (2007). A computational model for biofilm-based microbial fuel cells. *Water Research 41*, 2921-2940.

Pinto R., Srinivasan B., Manuel M., Tartakovsky B. (2010). A two-population bio-electrochemical model of a microbial fuel cell. *Bioresource Technology 101*, 5256-65.

Rozendal R., Hamelers H., Buisman C. (2006). Effects of Membrane Cation Transport on pH and Microbial Fuel Performance. *Environmental Science & Technology 40*, 5206-5211.

Sanchez-Herrera D., Pacheco-Catalán D., Valdez-Ojeda R., Canto-Canche B., Domínguez-Benetton X., Domínguez-Maldonado J., Alzate-Gaviria L. (2014). Characterization of anode and anolyte community growth and the impact of impedance in a microbial fuel cell. *BMC Biotechnology 14*, 1-10.

Torres C., Marcus A., Lee H., Parameswaran P., Krajmalnik-Brown R., Rittmann B. (2010). A kinetic perspective on extracellular electron transfer by anode-respiring bacteria. *FEMS Microbiology Reviews 34*, 3-17.

Torres C., Rittmann B.E., Marcus A.K. (2007). Conduction-based modeling of the biofilm anode of a microbial fuel cell. *Biotechnology & Bioengineering 98*, 1171-1182.

Valdez-Ojeda R., Aguilar-Espinosa M., Gómez-Roque L., Canto-Canché B., Escobedo Gracia-Medrano R.M., Domínguez- Maldonado J., Alzate-Gaviria L. (2014). Genetic identification of the bioanode and biocathode of a microbial electrolysis cell. *Revista Mexicana de Ingeniería Química 13*, 573-581.

Zeng Y., Choo Y.F., Kim B., Wu P. (2010). Modelling and simulation of two-chamber microbial fuel cell. *Journal Power Sources 195*, 79-89.

Zhang X., Halme A. (1995). Modelling of a microbial fuel cell process. *Biotechnology Letters 17*, 809-814.